*Micromachines* **2013**, *4*, 357-369; doi:10.3390/mi4040357

OPEN ACCESS

*micromachines*

**ISSN 2072-666X**

www.mdpi.com/journal/micromachines

*Article*

# Polydimethylsiloxane (PDMS) Sub-Micron Traps for Single-Cell Analysis of Bacteria

**Christopher Probst †, Alexander Grünberger †, Wolfgang Wiechert and Dietrich Kohlheyer ***

Institute of Bio- and Geosciences, IBG-1: Biotechnology, Forschungszentrum Jülich GmbH, D-52428 Jülich, Germany; E-Mails: c.probst@fz-juelich.de (C.P.); a.gruenberger@fz-juelich.de (A.G.); w.wiechert@fz-juelich.de (W.W.)

† These authors contributed equally to this work.

* Author to whom correspondence should be addressed; E-Mail: d.kohlheyer@fz-juelich.de; Tel.: +49-246-161-2927; Fax: +49-246-161-3870.

*Received: 25 July 2013; in revised form: 12 September 2013 / Accepted: 23 September 2013 / Published: 11 October 2013*

---

**Abstract:** Microfluidics has become an essential tool in single-cell analysis assays for gaining more accurate insights into cell behavior. Various microfluidics methods have been introduced facilitating single-cell analysis of a broad range of cell types. However, the study of prokaryotic cells such as *Escherichia coli* and others still faces the challenge of achieving proper single-cell immobilization simply due to their small size and often fast growth rates. Recently, new approaches were presented to investigate bacteria growing in monolayers and single-cell tracks under environmental control. This allows for high-resolution time-lapse observation of cell proliferation, cell morphology and fluorescence-coupled bioreporters. Inside microcolonies, interactions between nearby cells are likely and may cause interference during perturbation studies. In this paper, we present a microfluidic device containing hundred sub-micron sized trapping barrier structures for single *E. coli* cells. Descendant cells are rapidly washed away as well as components secreted by growing cells. Experiments show excellent growth rates, indicating high cell viability. Analyses of elongation and growth rates as well as morphology were successfully performed. This device will find application in prokaryotic single-cell studies under constant environment where by-product interference is undesired.

**Keywords:** microfluidics; single-cell analysis; *E. coli*; bacteria

---

## 1. Introduction

Single-cell analysis is a promising field for researchers from various disciplines as it holds potential for unraveling the intrinsic mechanisms of life with high accuracy. Investigations are performed on a single-cell basis rather than using typical bulk and average based measurements, which may mask conspicuous phenomena on the single-cell level. Therefore, microfluidics has become an essential part of the study of living microorganisms at small scale with spatial and temporal resolution, which would not be possible with conventional cytometric methods such as fluorescent activated cell sorting (FACS) and coulter counter.

Microfluidic single-cell analysis assays can be divided into two main categories, namely studying either the whole cell (growth [1], morphology [2], or fluorescent bioreporters [3,4]) or its lysate (genome, transcriptome, proteome and metabolome) [5]. Emerging technologies such as genetically encoded bioreporters have extended the toolbox for noninvasive whole-cell single-cell analysis and have been applied to measure metabolic states such as intercellular pH [6] and product formation [3].

Recently, two main microfluidic cultivation principles for single cells were exploited, namely:

(i) the cultivation of single mother cells growing into discrete isogenic microcolonies [2,7,8] and
(ii) arrays of physically separated individual cells and cell tracks [9,10].

In microcolonies, individual cells may be exposed to extracellular stimuli from neighboring cells, for example due to secreted metabolites or environmental gradients within the microcolony [11]. However, when performing perturbation studies to analyze single-cell responses, avoiding such community effects becomes essential.

Various physical principles have been applied to immobilize individual cells by means of, for example, single droplets [12,13], acoustic waves [14], electrophoretic forces [15–20], optical tweezers [21] or mechanical objects and structures [22]. Most of these single-cell trapping methods require laborious setups and may impact on the entrapped cells through temperature gradients or the formation of oxygen radicals [23], for example.

Alternatively, mechanical barriers and trapping structures inducing hydrodynamic forces on the cell enable the fast and reliable immobilization of hundreds of cells in parallel [9]. Single cells were entrapped in arrays of cup-shaped barrier structures with the openings facing towards the flow direction. Simultaneous cell pairing and the fusion of large arrays of cells were realized in [10] using the same passive cell-trapping approach. Instead of barrier structures, single cells can also be immobilized using rejoined gaps, where a meander-shaped channel is interconnected at multiple points by narrow junctions along its length [24]. The difference in the hydraulic resistance of the channels forces single cells into the narrow channels, where they become entrapped. The immobilization realized by both approaches is a statistical process and does not allow for a specific cell to be taken out of the flow or released again. More active control over the immobilization was achieved by applying negative pressure in order to pull cells into narrow channels arranged along the channel walls [25–28]. Throughput is typically decreased by better spatial control over the single cells.

Despite the many advantages of these methods, all of them share the same limitation concerning cell size and shape. Previous work was carried out mainly with large mammalian cells or spherical eukaryotic cells such as yeast. Efforts have been made to apply identical concepts for immobilizing

bacteria, for example *Escherichia coli*. Obviously, their small size (10 times smaller than yeast) and typically rod-shaped morphology make it difficult to immobilize them precisely [29]. Most concepts lack the possibility of removing the surplus of daughter cells once a single mother cell divides, leading to larger colonies after cell division. As microbial growth is often faster than eukaryotic cell growth, a reliable microbial single-cell analysis system necessitates the continuous removal of daughter cells.

To enable long-term analysis, the so-called "mother machine" was utilized to immobilize and cultivate hundreds of *E. coli* mother cells in narrow dead-end channels with a height of 1 μm [30]. At the end of each channel, the proliferating mother cell was observed over several hours as well as multiple generations of its descendants before cells were pushed out of the channel and flushed away. The mother machine concept is well suited for cell aging studies as the old pole mother cell remains at a fixed position. However, accumulation of secreted products inside the dead-end channels and concentration gradients might still cause cell–cell heterogeneity in more complex assays. A similar approach was reported by [11,31] in which parallel growth channels with two openings facing the media supply streams were used to cultivate single cells. As single cells grew towards both openings of the tracks, the device was not suited for cell aging studies. In contrast, a balanced culture was maintained over multiple generations. Instead of PDMS, [11] applied porous agarose as chip material to allow diffusion between each of the growth channels. Indeed, this was proven through the successful co-cultivation of two dependent *E. coli* auxotrophs that can complement the amino acid deficiencies of one another [11]. Due to the agarose material, concentration gradients may lead to inhomogeneous cultivation conditions. Inoculation of mother cells was achieved by simply pipetting a cell suspension onto the bottom glass slide of the device, before placing the agarose perfusion chip with incorporated growth channels on top of it. Instead, [31] applied PDMS as chip material, not facilitating diffusion between the growth channels. However, cell–cell interactions and accumulation of secreted products may occur inside the densely packed growth channels. In [31], device cell seeding was achieved by an imbalance of the two media volume flows inside the main channels actively pushing the mother cells into the tracks.

This article outlines the fabrication and characterization of sub-micron sized single-cell traps for the cultivation and analysis of individual bacteria located inside a continuous media flow. High-resolution electron-beam-written photolithography masks were utilized to fabricate SU-8 molds with 300–400 nm structural resolution with the approximate size of typical bacteria and smaller. Polydimethylsiloxane (PDMS) replication was performed to fabricate single-use chip devices, thereby replicating the sub-micron SU-8 trapping structures well. *E. coli* MG1655 cells were immobilized simply by flow inside the single-cell traps, cultivated, and observed by time-lapse microscopy over several hours. Division times at 20 min demonstrated excellent cell viability. Due to the fast media flow towards and around the traps, side products secreted by the cells were rapidly washed away without affecting any other cells further downstream. Supporting flow profile analysis was performed using computational fluidic dynamics. The present system will be used for single-bacteria perturbation studies.

## 2. Experimental

### *2.1. Soft Lithography*

A video-based description of a comparable fabrication method can be found in [32]. Microfluidic master molds were fabricated using the negative photoresist SU-8 (MicroChem, Newton, MA, USA). Prior to resist deposition, a 4-inch silicon wafer was cleaned with piranha solution followed by hydrofluoric acid and rinsed with DI water. After dry spinning, the substrate was dehydrated for 20 min at 200 °C. For the first layer of photoresist, a mixture of two different SU-8 photoresists was used to achieve the designated height of 1 µm. The photoresists SU-8 2000.5 and SU-8 2010 were mixed in a ratio of 24:88, with a total weight of 60 g. This mixture was spin-coated onto the substrate at 500 rpm with an acceleration of 100 rpm/s for 10 s and at 2000 rpm with an acceleration of 300 rpm/s for 30 s. Soft bake was performed at 65 °C for 90 s, at 95 °C for 90 s and at 65 °C for 60 s. Afterwards, the substrate was exposed (7 mW/cm²) for 3 s using a mask aligner (MA-6, SUSS MicroTec, Garching, Germany) and an electron-beam-written chromium dark-field mask. Post-exposure bake was carried out at 65 °C for 60 s and 95 °C for 60 s. Unexposed parts of the photoresist were dissolved by immersing the substrate in developer solution (mr-DEV 600, micro resist technology GmbH, Berlin, Germany) for 60 s, then again in fresh developer solution for 40 s, and dipping it in isopropanol for 20 s. Developed substrates were dried and hard-baked for 10 min at 150 °C.

The second layer was coated with the negative photoresist SU-8 2010 at 500 rpm with an acceleration of 100 rpm/s for 10 s and 4000 rpm with an acceleration of 300 rpm/s for 30 s. After the deposition, the substrate was baked at 65 °C for 15 min and at 95 °C for 60 min. The photoresist was exposed (7 mW/cm²) for 12 s using a mask aligner (MA-6, SUSS MicroTec, Garching, Germany) and an electron-beam-written chromium dark-field mask. Post-exposure bake was carried out at 65 °C for 5 min and at 95 °C for 3 min. The development was carried out as described for the first layer. Finally, the structures were hard-baked for 6 h at 150 °C.

PDMS replicas were fabricated by pouring a 10:1 mixture of PDMS (Sylgard 184, Dow Corning, Midland, MI, USA) onto the wafer and baking it at 80 °C for 90 min. Next, the PDMS slab was peeled off the wafer and cut into separate chips. The chips were washed in n-pentane for 90 min to remove monomer residue and then transferred to an acetone bath for 90 min to remove the n-pentane. The chips were dried overnight. Prior to the experiments, each chip was thoroughly cleaned with acetone, isopropanol and, after drying, with scotch tape to remove any dust particles that may have clung to it. For high-resolution microscopy, a cleaned chip was bonded onto a 170 µm thin glass cover slip using an oxygen plasma generator (Diener electronic GmbH, Ebhausen, Germany).

### *2.2. Sample Preparation*

*E. coli* (MG1655) was pre-cultured in 20 mL of fresh LB medium in 100 mL shake flasks and cultivated at 37 °C and 150 rpm overnight. 25 µL of the overnight culture was transferred to 20 mL of fresh LB and grown until an optical density (OD 600, BioPhotometer plus, Eppendorf AG, Hamburg, Germany) of 1 was reached. Afterwards, 100 µL of the main culture was diluted in 900 µL of fresh LB medium prior to inoculation into the microfluidic device.

### *2.3. Experimental Procedure*

*E. coli* cells were inoculated into single-cell trapping arrays and cultivated for 4 h. Cells were entrapped by infusing the cell suspension through the main channel until the traps were filled with single cells. Afterwards, the main channel was continuously flushed with fresh growth medium (200 nL/min) to remove excessive cells and ensure constant environmental conditions. Cells were grown at 37 °C using an in-house developed incubator mounted to a motorized microscope (Ti Eclipse, Nikon, Tokyo, Japan). Time-lapse images of immobilized cells were taken at 5 min intervals and analyzed using the commercially available software suit NIS-Elements.

## 3. Results and Discussion

### *3.1. Trap Layout and Geometry*

Due to the typical size of *E. coli* (≈500 nm diameter and ≈2 μm length), the various concepts for the immobilization of single eukaryotic cells that have been demonstrated in other studies do not work properly for *E. coli*. However, [9] laid the foundation for microfluidic barrier trapping structures. In a first approach, we miniaturized the existing concepts for barrier structures down to the size of single *E. coli*. Our microfluidic device incorporates two key elements, namely:

(i) the main channels for cell suspension and growth media supply, with a height of 10 μm (Figure 1a), and
(ii) the cultivation area containing barrier structures for cell entrapment with a height between 800 nm and 1 μm, as depicted in Figure 1b.

A cell suspension was flushed through the main channel to inject single bacteria into the traps. The barrier structures developed by [9] allowed fluid flow to pass over the structures between PDMS and glass. This principle was not possible in our approach as bacteria tend to grow into narrow gaps [33].

Initial experiments with this newly developed single-cell trapping method revealed that clogging occurred through unspecific adhesion of the cells during the filling process as well as during cultivation (Figure 1c). Cells became trapped before reaching the gap of the trapping region or adhered to the glass slide inside the 1 μm channel. This shows that systems which were initially developed for eukaryotic cells cannot simply be scaled down to match conditions for single-bacteria analysis. In particular, the handling of different shapes and the removal of daughter cells that appear have to be considered.

In a second approach, the trapping region was improved by reducing the plateau area to minimize clogging and unspecific adhesion, enabling cells to flow by without getting stuck (Figure 2a). Nevertheless, further experiments showed that this alteration did not prevent the adhesion of cells outside of the barrier structures. Finally, the trapping region was reduced to a round pillar with a height of 9 μm and a diameter of 17 μm (Figure 2b). This change allowed the successful immobilization of single *E. coli* cells without undesirable adhesion during the filling process and during cell growth. After division, daughter cells were immediately removed from the trapping region and washed away with the media stream.

**Figure 1.** (**a**) Immobilization of single bacteria into a trapping array. (**b**) SEM images of trapping region containing several trapping structures for the immobilization of single bacteria. (**c**) Unspecific adhesion of *E. coli* leading to crowded growth in first single-cell trapping concept.

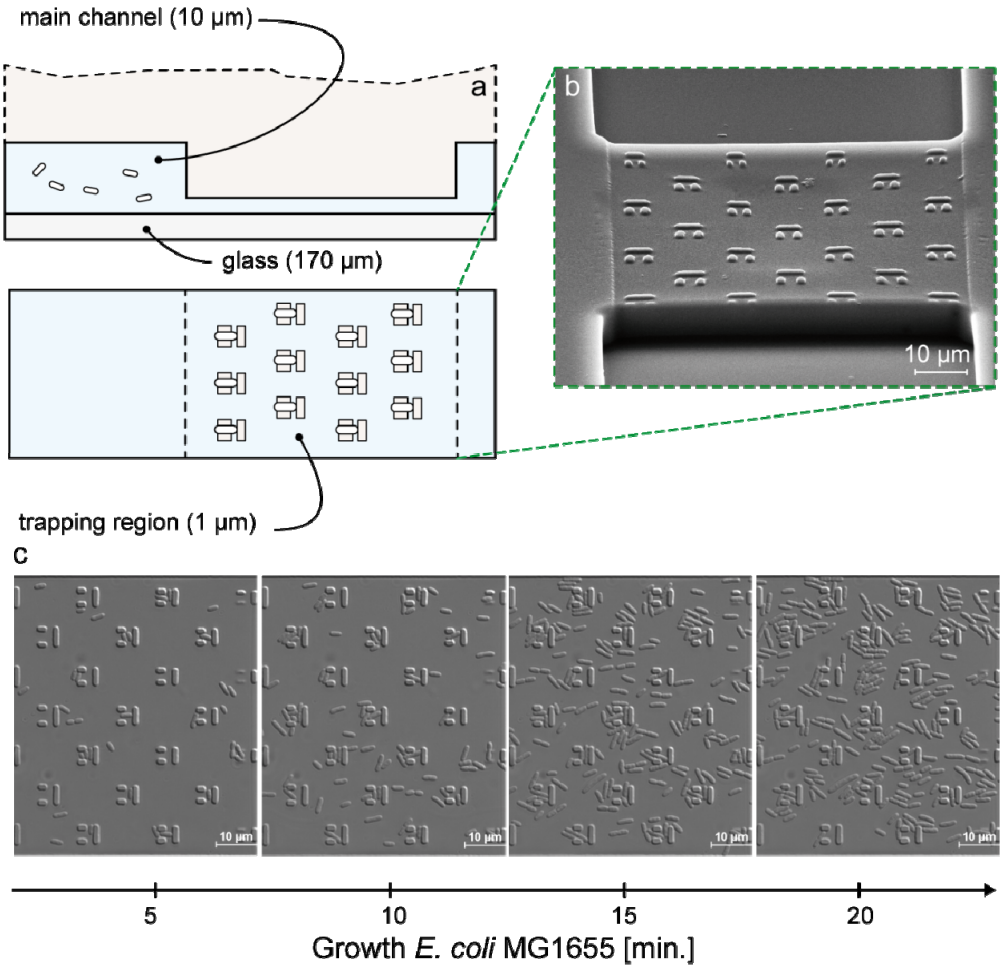


**Figure 2.** (**a**) SEM image of single-cell trapping structures with partially reduced trapping area. (**b**) SEM image of final trapping structure.

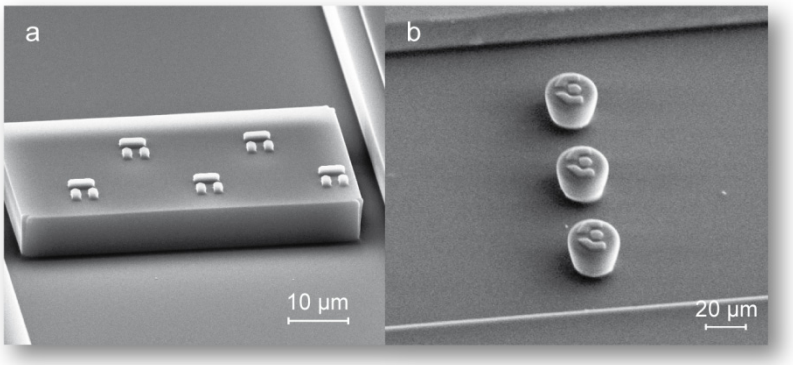


Single-cell studies presented in this paper were carried out using two types of barrier structures as depicted in Figure 3. The first design allows one cell at a time to be immobilized (Figure 3a) inside a 1.5 µm wide gap formed by three rectangular barriers with a width of 2 µm and a height of 1 µm.

The second design allows two cells to be trapped simultaneously, increasing the throughput compared to the first structure, which allows single-cell trapping only. The gap between the barrier structures is 1 µm in width and 1 µm in length. The constriction at the end of each gap is 500 nm in width (Figure 3b).

In contrast to previously published single-bacteria analysis devices by [11,30,31], our system facilitates fast and efficient inoculation by simply injecting the cell suspension. In fact, within a few seconds of perfusion, a good number of traps were inoculated, each with a single cell. The current proof-of concept chip contained 45 single traps and 42 double traps resulting in a loading capacity of individual 129 bacteria. As shown in Figure 3b, 60% of the single-traps and 87% of the double-traps were occupied within 20 s.

Experiments showed that despite the small dimensions between the barrier structures of design (a), *E. coli* was still able to grow through the barrier structure. Better results were achieved with design (b), where the additional constriction of 500 nm at the end of each gap restricted growth to the front inlet direction.

**Figure 3.** (**a**) Sub-micron single-cell trapping structures used for the successful immobilization and cultivation of *E. coli*. (**b**) Comparison of the number of trapped cells in single and double cell traps. After flushing the device with the cell suspension for a couple of seconds, 60% of the single traps and 87% of double traps were filled.

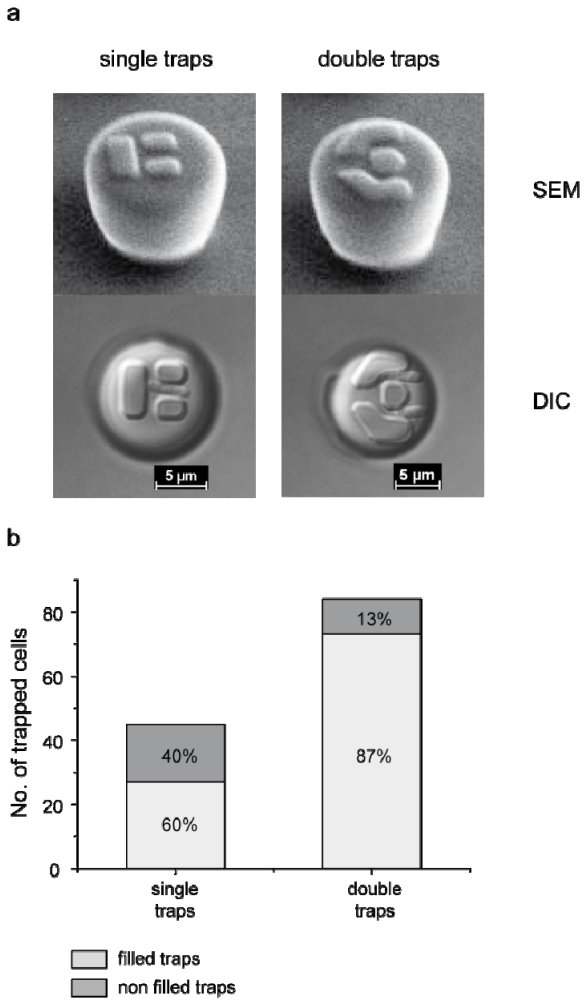

### *3.2. Numerical Simulation*

Numerical simulations were conducted using COMSOL Multiphysics to analyze the fluid flow inside and around the single-cell trapping structures. Figure 4a shows the model geometry used in all simulations with a total length of 100 µm, width of 100 µm and height of 10 µm. The inlet boundary was defined to have a volumetric velocity of 16.67 × $10^{-12}$ $m^3/s$, corresponding to a flow rate of 1000 nL/min in our system, which equals the flow rate used for cell inoculation during experiments. The outlet boundary was set to a gauge pressure of 0 Pa. All other surfaces of the geometry were defined as walls with a no-slip condition.

Reduction of the channel height (1 µm) near the trapping structure led to a drastic 1000 fold increase in the hydraulic resistance and much lower velocity inside the traps (Figure 4c) compared to the neighboring regions of the channel with an overall height of 10 µm (Figure 4b). Once a single cell is trapped, the flow is forced to diverge and flow around the trapping structure instead of flowing through the structure, and cannot trap any additional cells. This guarantees that only one cell at a time is trapped. Due to the reduced area of the shallow space surrounding the trapping structure, no additional cells can be caught in front. Furthermore, due to a higher convective flow around the trapping structure, by-products and surplus cells are washed away continuously, maintaining constant conditions over time.

**Figure 4.** (**a**) Geometry used for numerical simulation with an inlet flow rate of 1000 nL/min, outlet gauge pressure 0 Pa and walls defined as no-slip walls. (**b**) Flow profile and velocity distribution along the whole microfluidic channel. (**c**) Distribution of flow velocity in the shallow region surrounding the trapping structure.

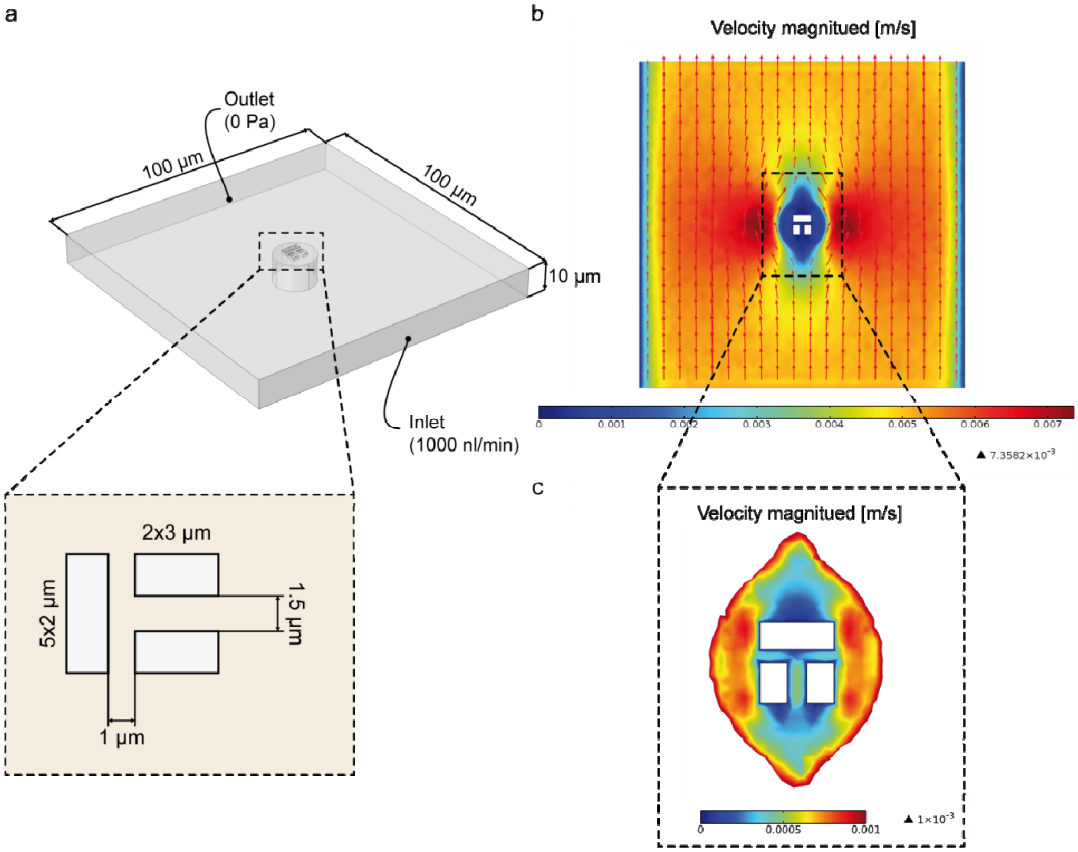

### *3.3. Single Cell Cultivation*

Growth and morphology are key viability indicators in microbiology [34]. Single-cell growth assays analyzing division time and morphology were used in the present approach to validate our device. As shown in Figure 5a, we measured the cell length from one individual *E. coli* over 300 min cultivation by manually analyzing recorded time-lapse images. Division times as well as cell elongation rates were obtained. For analysis, a linear curve was fitted to the cell length over each generation period as illustrated in Figure 5d. The slope of each fit represents the respective elongation rate, as shown in Figure 5b.

**Figure 5.** (**a**,**b**) Single-cell traces (cell length, division time and elongation rate) of one distinct *E. coli* mother cell. (**c**) Time-lapse image series showing the successful removal of a "daughter" cell from the trap during cultivation. (**d**) Cell length over the 30 min of cultivation describing the determination of the division time as well as the elongation rate.

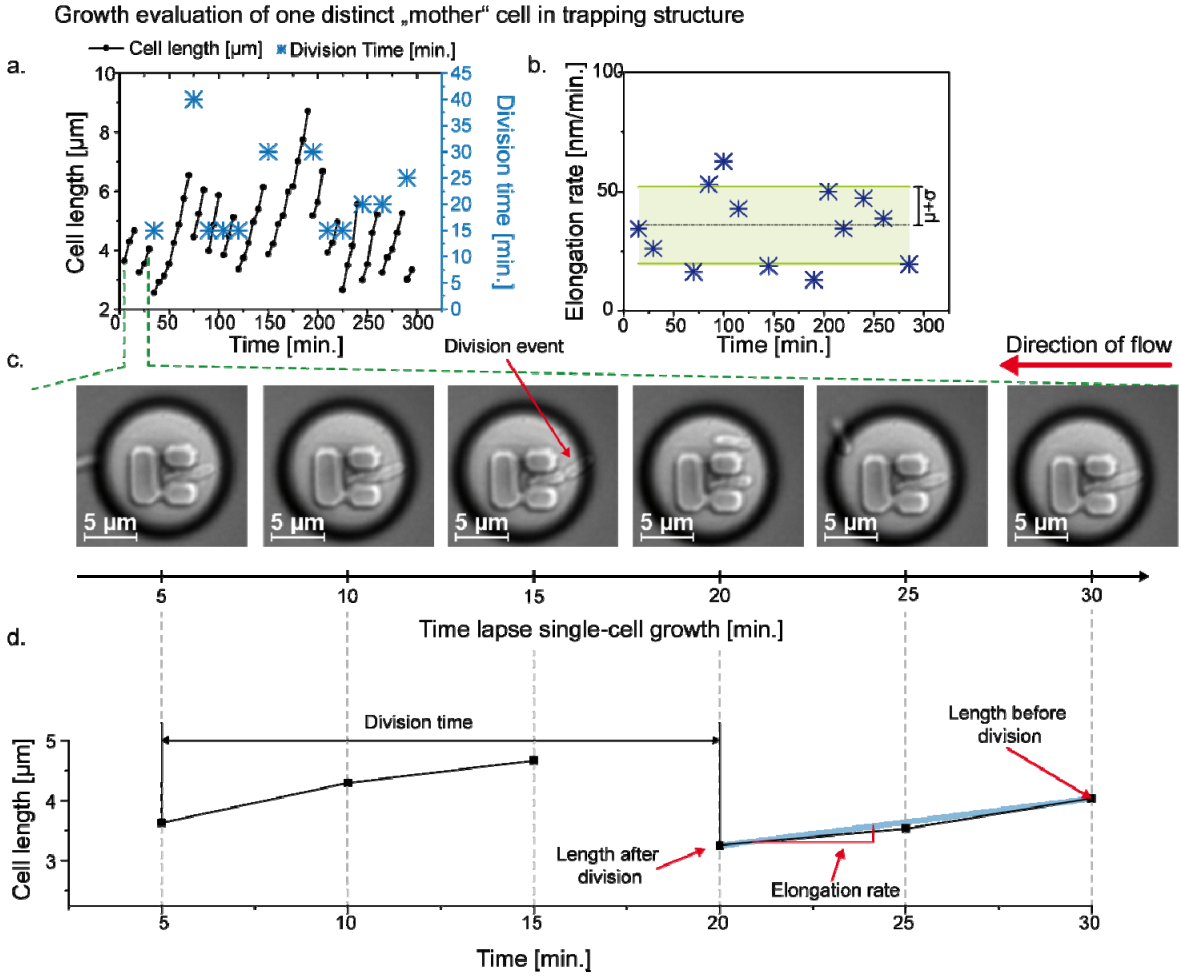


By averaging the division time of single cells in multiple single-cell trapping arrays (Figure 5b), we derived a 20 min division time of *E. coli*, which corresponds well to previously reported results [11,30]. Division times were derived by manual image analysis, as depicted Figure 5c,d. The time-lapse image in which both cells were apparently separated by a visible septum, was considered as the division end. Obviously, the higher the image frequency during time-lapse microscopy, the more

accurate the division time could be evaluated. In our experiments, we found the time-lapse imaging frequency of 5 min as a reasonable compromise between total throughput and accuracy of analysis.

The mean division time and standard deviation were calculated over at least 9 generations from five traps, respectively (Figure 6a). Longer division times can be explained by the appearance of filaments, a well-known phenomenon in many microbial organisms often induced by cell stress [35]. Filamentation leads to much longer cells and delays the division event. However, by evaluating cell length before ($L_{\text{Before}}$) and after ($L_{\text{After}}$) division, we observed an almost Gaussian distribution (Figure 6b). Filamentation only occurred in a few instances and was mainly observed directly after the seeding of the single-cell trapping structures. After the first division, the filamentous cells reverted to normal growth behavior with an average $L_{\text{Before}}$ = 5 µm and $L_{\text{After}}$ = 3 µm. The Gaussian distribution was validated by using the Kolmogorov-Smirnov test (goodness of fit). As it can be seen in Figure 6b, for a significance level of α = 0.05 and a critical value $d$ = 0.174 ($n$ = 61) it was found that $D_{\text{after}}$ = 0.094 ($p$-value = 0.643) and $D_{\text{before}}$ = 0.085 ($p$-value = 0.781). Since both values are smaller than the critical value $d$, we concluded that they are evenly distributed. Thus, we can presume that our newly developed method is suitable for the cultivation and analysis of single-cells such as *E. coli*.

**Figure 6.** (**a**) Average division time of 20 min derived from 5 single-cell trapping structures over the whole cultivation period of 300 min. (**b**) Average cell length distribution before ($L_{\text{Before}}$ ≈ 5 µm) and after ($L_{\text{After}}$ ≈ 3 µm) division of all analyzed traps, showing a nearly Gaussian distribution.

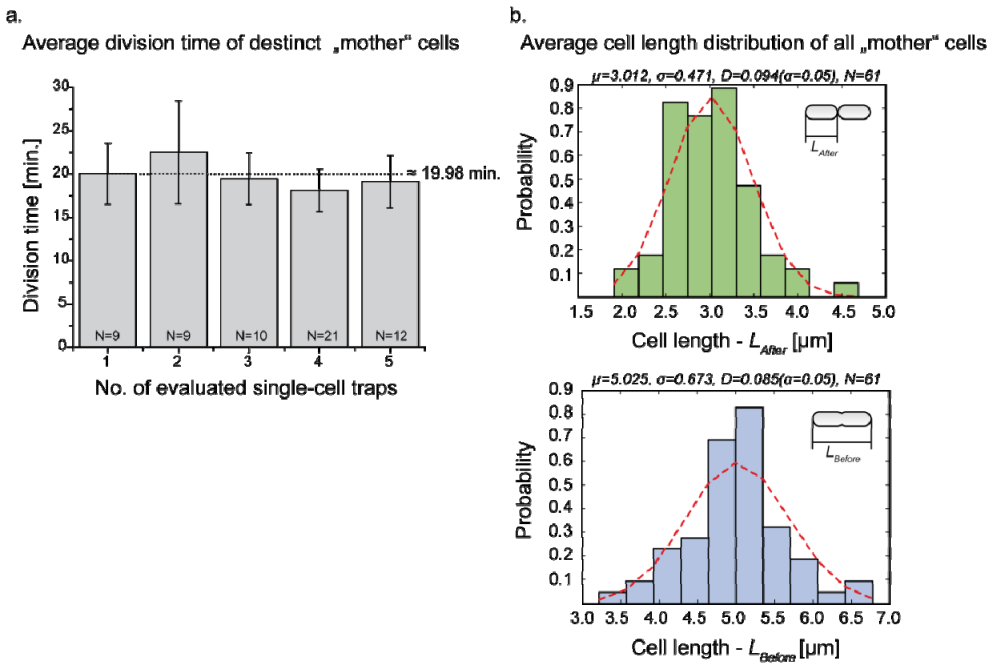


## 4. Conclusions

Microfluidics has emerged as a powerful tool in single-cell analysis, with a wide spectrum of different applications. However, many microfluidic systems for single whole-cell analysis are restricted by the size of the organisms (mammalian cells or eukaryotic cells such as yeast) that can be cultivated. In the present article, we presented a microfluidic device containing sub-micron sized

single-cell traps for the immobilization and cultivation of individual bacteria, successfully demonstrated with *E. coli*. Furthermore, a simple loading procedure was established in which simply the cell suspension is perfused through the media supply channel filling the traps with a good efficiency and reproducibility within a few seconds. Barrier structures with sub-micron sized channel geometry allowed for the trapping of single rod-shaped *E. coli*. The layout ensured that neighboring cells and by-products were continuously removed by a fast media flow maintaining constant conditions. We cultivated *E. coli* cells over several hours showing constant division times and typically rod-shaped morphology, indicating good viability. Our findings form the basis for further single-bacteria analysis under constant environmental conditions without neighboring cells affecting each other. In future applications, our device is going to be applied for analyzing extracellular and intracellular responses of single bacteria due to short term fluctuations in pH, temperature, carbon sources and others. This will be achieved, e.g., by the application of genetically encoded fluorescence sensors [3,4]. The layout can be applied to many other types of typically rod-shaped bacteria of similar size.

## Acknowledgments

This work was performed in part at the Helmholtz Nanoelectronic Facility (HNF) of Forschungszentrum Jülich GmbH. The authors would like to thank all those at HNF for their help and support.

## Conflicts of Interest

The authors declare no conflict of interest.

## References

1. Grünberger, A.; van Ooyen, J.; Paczia, N.; Rohe, P.; Schiendzielorz, G.; Eggeling, L.; Wiechert, W.; Kohlheyer, D.; Noack, S. Beyond growth rate 0.6: Corynebacterium glutamicum cultivated in highly diluted environments. *Biotechnol. Bioeng.* **2013**, *110*, 220–228.
2. Grunberger, A.; Paczia, N.; Probst, C.; Schendzielorz, G.; Eggeling, L.; Noack, S.; Wiechert, W.; Kohlheyer, D. A disposable picolitre bioreactor for cultivation and investigation of industrially relevant bacteria on the single cell level. *Lab Chip* **2012**, *12*, 2060–2068.
3. Mustafi, N.; Grünberger, A.; Kohlheyer, D.; Bott, M.; Frunzke, J. The development and application of a single-cell biosensor for the detection of l-methionine and branched-chain amino acids. *Metab. Eng.* **2012**, *14*, 449–457.
4. Schendzielorz, G.; Dippong, M.; Grünberger, A.; Kohlheyer, D.; Yoshida, A.; Binder, S.; Nishiyama, C.; Nishiyama, M.; Bott, M.; Eggeling, L. Taking control over control: Use of product sensing in single cells to remove flux control at key enzymes in biosynthesis pathways. *ACS Synth. Biol.* **2013**, doi:10.1021/sb400059y.
5. Yin, H.; Marshall, D. Microfluidics for single cell analysis. *Curr. Opin. Biotech.* **2012**, *23*, 110–119.
6. Miesenbock, G.; de Angelis, D.A.; Rothman, J.E. Visualizing secretion and synaptic transmission with pH-sensitive green fluorescent proteins. *Nature* **1998**, *394*, 192–195.

7. Prindle, A.; Samayoa, P.; Razinkov, I.; Danino, T.; Tsimring, L.S.; Hasty, J. A sensing array of radically coupled genetic "biopixels". *Nature* **2012**, *481*, 39–44.
8. Groisman, A.; Lobo, C.; Cho, H.; Campbell, J.K.; Dufour, Y.S.; Stevens, A.M.; Levchenko, A. A microfluidic chemostat for experiments with bacterial and yeast cells. *Nat. Meth.* **2005**, *2*, 685–689.
9. Di Carlo, D.; Aghdam, N.; Lee, L.P. Single-cell enzyme concentrations, kinetics, and inhibition analysis using high-density hydrodynamic cell isolation arrays. *Anal. Chem.* **2006**, *78*, 4925–4930.
10. Skelley, A.M.; Kirak, O.; Suh, H.; Jaenisch, R.; Voldman, J. Microfluidic control of cell pairing and fusion. *Nat. Methods* **2009**, *6*, 147–152.
11. Moffitt, J.R.; Lee, J.B.; Cluzel, P. The single-cell chemostat: an agarose-based, microfluidic device for high-throughput, single-cell studies of bacteria and bacterial communities. *Lab Chip* **2012**, *12*, 1487–1494.
12. Brouzes, E.; Medkova, M.; Savenelli, N.; Marran, D.; Twardowski, M.; Hutchison, J.B.; Rothberg, J.M.; Link, D.R.; Perrimon, N.; Samuels, M.L. Droplet microfluidic technology for single-cell high-throughput screening. *P. Natl. Acad. Sci.* **2009**, *106*, 14195–14200.
13. Choi, K.; Ng, A.H.C.; Fobel, R.; Wheeler, A.R. Digital Microfluidics. *Annu. Rev. Anal. Chem.* **2012**, *5*, 413–440.
14. Ding, X.; Lin, S.-C.S.; Kiraly, B.; Yue, H.; Li, S.; Chiang, I.-K.; Shi, J.; Benkovic, S.J.; Huang, T.J. On-chip manipulation of single microparticles, cells, and organisms using surface acoustic waves. *P. Natl. Acad. Sci.* **2012**.
15. Chiou, P.Y.; Ohta, A.T.; Wu, M.C. Massively parallel manipulation of single cells and microparticles using optical images. *Nature* **2005**, *436*, 370–372.
16. Dusny, C.; Fritzsch, F.S.O.; Frick, O.; Schmid, A. Isolated microbial single cells and resulting micropopulations grow faster in controlled environments. *Appl. Environ. Microbiol.* **2012**, *78*, 7132–7136.
17. Fritzsch, F.S.O.; Rosenthal, K.; Kampert, A.; Howitz, S.; Dusny, C.; Blank, L.M.; Schmid, A. Picoliter nDEP traps enable time-resolved contactless single bacterial cell analysis in controlled microenvironments. *Lab Chip* **2013**, *13*, 397–408.
18. Hsu, H.-y.; Ohta, A.T.; Chiou, P.-Y.; Jamshidi, A.; Neale, S.L.; Wu, M.C. Phototransistor-based optoelectronic tweezers for dynamic cell manipulation in cell culture media. *Lab Chip* **2010**, *10*, 165–172.
19. Kortmann, H.; Chasanis, P.; Blank, L.M.; Franzke, J.; Kenig, E.Y.; Schmid, A. The envirostat—A new bioreactor concept. *Lab Chip* **2009**, *9*, 576–585.
20. Kim, S.H.; Yamamoto, T.; Fourmy, D.; Fujii, T. Electroactive microwell arrays for highly efficient single-cell trapping and analysis. *Small* **2011**, *7*, 3239–3247.
21. Ramser, K.; Hanstorp, D. Optical manipulation for single-cell studies. *J. Biophotonics* **2010**, *3*, 187–206.
22. Johann, R.M. Cell trapping in microfluidic chips. *Anal. Bioanal Chem* **2006**, *385*, 408–412.
23. Svoboda, K.; Block, S.M. Biological applications of optical forces. *Annu. Rev. Biophys. Biomed. Struct.* **1994**, *23*, 247–285.
24. Kobel, S.; Valero, A.; Latt, J.; Renaud, P.; Lutolf, M. Optimization of microfluidic single cell trapping for long-term on-chip culture. *Lab Chip* **2010**, *10*, 857–863.

25. Khine, M.; Lau, A.; Ionescu-Zanetti, C.; Seo, J.; Lee, L.P. A single cell electroporation chip. *Lab Chip* **2005**, *5*, 38–43.
26. Lee, P.J.; Hung, P.J.; Shaw, R.; Jan, L.; Lee, L.P. Microfluidic application-specific integrated device for monitoring direct cell–cell communication via gap junctions between individual cell pairs. *Appl. Phys. Lett.* **2005**, *86*, 223902, doi:10.1063/1.1938253.
27. Valero, A.; Post, J.N.; van Nieuwkasteele, J.W.; ter Braak, P.M.; Kruijer, W.; van den Berg, A. Gene transfer and protein dynamics in stem cells using single cell electroporation in a microfluidic device. *Lab Chip* **2008**, *8*, 62–67.
28. Zhu, Z.; Frey, O.; Ottoz, D.S.; Rudolf, F.; Hierlemann, A. Microfluidic single-cell cultivation chip with controllable immobilization and selective release of yeast cells. *Lab Chip* **2012**, *12*, 906–915.
29. Kim, M.-C.; Isenberg, B.C.; Sutin, J.; Meller, A.; Wong, J.Y.; Klapperich, C.M. Programmed trapping of individual bacteria using micrometre-size sieves. *Lab Chip* **2011**, *11*, 1089–1095.
30. Wang, P.; Robert, L.; Pelletier, J.; Dang, W.L.; Taddei, F.; Wright, A.; Jun, S. Robust growth of escherichia coli. *Curr. Biol.* **2010**, *20*, 1099–1103.
31. Long, Z.; Nugent, E.; Javer, A.; Cicuta, P.; Sclavi, B.; Cosentino Lagomarsino, M.; Dorfman, K.D. Microfluidic chemostat for measuring single cell dynamics in bacteria. *Lab Chip* **2013**, *13*, 947–954.
32. Gruenberger, A., Probst, C., Heyer, A., Wiechert, W., Frunzke, J., Kohlheyer, D. Microfluidic picoliter bioreactor for microbial single-cell analysis: Fabrication, system setup and operation. *J. Vis. Exp.* **2013**, doi:10.3791/50560.
33. Männik, J.; Driessen, R.; Galajda, P.; Keymer, J.E.; Dekker, C. Bacterial growth and motility in sub-micron constrictions. *P. Natl. Acad. Sci.* **2009**, *106*, 14861–14866.
34. Lecault, V.; White, A.K.; Singhal, A.; Hansen, C.L. Microfluidic single cell analysis: From promise to practice. *Curr. Opin. Chem. Biol.* **2012**, *16*, 381–390.
35. Justice, S.S.; Hunstad, D.A.; Cegelski, L.; Hultgren, S.J. Morphological plasticity as a bacterial survival strategy. *Nat. Rev. Micro.* **2008**, *6*, 162–168.

© 2013 by the authors; licensee MDPI, Basel, Switzerland. This article is an open access article distributed under the terms and conditions of the Creative Commons Attribution license (http://creativecommons.org/licenses/by/3.0/).